Simulation of the Concomitant Nuclear Reactions Contribution to the Actinide Photofission on the M-30 Microtron at 17.5 MeV Bremsstrahlung Energy

Eugene Oleinikov[*], Igor Pylypchynets, Oleg Parlag

Institute of Electron Physics, Universitetska 21, Uzhgorod, Ukraine

Abstract   To stimulate the actinide photofission reaction, bremsstrahlung beams obtained at electron accelerators are used, which, in addition to photons, contain residual electrons and secondary photoneutrons. When interacting with the studied actinide samples, residual electrons and secondary photoneutrons can initiate accompanying nuclear reactions: electrofission and fission by fast neutrons. As a result of the simulations, the contributions of the specified concomitant reactions to the photofission of actinides ^{232}Th, ^{238}U, and ^{239}Pu were determined upon their activation at the M-30 microtron electron accelerator for a fixed initial electron energy of 17.5 MeV. It was established that the contribution of the specified concomitant reaction outputs to the photofission reaction outputs of ^{232}Th, ^{238}U, and ^{239}Pu does not exceed 1% for the proposed stimulation scheme on the M-30 microtron. The obtained results can be used to develop optimal actinide activation schemes for various types of electron accelerators when studying their nuclear-physical characteristics.

Keywords   Concomitant nuclear reactions, Actinide fission yields, GEANT4 toolkit

1. Introduction

From the moment of the discovery of photofission to the present day, it has been intensively researched both from a theoretical point of view and for practical application. The characteristics of actinides photofission reactions (in which, after absorption of a photon, the nucleus splits into two or more fragments) provide essential information about the properties of atomic nuclei [1,2]. This especially applies to the data on the yields of fragments, prompt and delayed neutrons, which are formed in the process of photofission of actinides ^{232}Th, ^{238}U, ^{239}Pu. Information about their characteristics is necessary for solving a wide range of applied problems of nuclear technology (non-destructive methods of isotope analysis of fissionable and non-fissionable nuclear materials [3,4], controlled subcritical systems [5,6] alternative production of medical radioisotopes [7,8], analysis of actinide content in ecological and biological samples [9]).

The actinides photofission reaction is stimulated by bremsstrahlung beams [3,4,10,11] and monoenergetic photons formed as a result of nuclear reactions (for example (p,γ), (n,γ)) [12,13] and Compton backscattering [14]. The use of beams of monoenergetic photons to study the characteristics of photofission is quite limited due to the technical difficulties of obtaining them. Therefore, bremsstrahlung beams (high-energy photons with spectra of a continuous energy distribution), obtained at electron accelerators, are the primary tool in studying actinides photofission [1].

Converters (materials with a high mass number) are used to convert electron beams into bremsstrahlung radiation at electron accelerators. The maximum output of bremsstrahlung is achieved when the converter thickness is less than the electron's mean free path in it [15,16]. Therefore, residual electrons will be present in the bremsstrahlung beam, which, when interacting with actinides, can initiate concomitant electrofission reactions in the studied samples. During the interaction of electrons with the converter material, in addition to reactions along the $e \to \gamma$ and $e \to \gamma \to n$ channels, nuclear reactions of the $e \to n$ type occur, which lead to the formation of photoneutrons of a continuous energy spectrum (commonly, prompt neutrons) [17,18], and can additionally initiate neutron reactions [19].

These factors can significantly affect the results of studies of the actinides' photofission characteristics. In this regard (when in the sample activation schemes on electronic accelerators, deflecting magnets are not used to divert electrons that have passed through the converter [20]), there is a need to "clean" bremsstrahlung beams from residual electrons and secondary photoneutrons. "Cleaning" of bremsstrahlung beams, without weakening the intensity of photons, is carried out using filters [21].

A key component of obtaining accurate data on the yields of photofission products of actinides is the accurate determination of the number of fission events that occur during their irradiation for various activation schemes during experimental studies. This requires information on the integral values of the photon fluxes close to the spectra energies from the photofission reaction's thresholds to their maximum values, which strongly depend on the energies and spatial distributions of the primary electron beams, their fluctuations, and activation schemes [18,22,23]. In addition, reliable information is needed about the spectra of residual electrons and secondary photoneutrons and their integral values, which are present in the bremsstrahlung beam and can stimulate concomitant nuclear reactions (electro- and neutron fission).

To obtain information about the characteristics of bremsstrahlung beams and their constituent components (photons, residual electrons, secondary photoneutrons) generated on electron accelerators (taking into account their design features) and sample irradiation schemes, computer simulation using the GEANT4 Monte Carlo software code is widely used [18,21,22].

GEANT4 [24] makes it possible to model the spectra of photons, residual electrons, and secondary photoneutrons as closely as possible to the actual conditions of their formation, which are necessary for calculating the contribution of the outputs of concomitant nuclear reactions to the yield of the actinide photofission reaction when they are irradiated at electron accelerators.

The current work aimed to evaluate the contribution of concomitant nuclear reactions (electron and neutron fission) to the photofission reaction yields of actinides ^{232}Th, ^{238}U, and ^{239}Pu irradiated at the electron accelerator of the Institute of Electronic Physics of the National Academy of Sciences of Ukraine - the M-30 microtron for the optimal sample activation scheme, proposed in our previous work [22].

To implement the given task, the spectra of photons, residual electrons, and photoneutrons interacting with the investigated actinide samples (taking into account their nuclear-physical characteristics) were modeled, which were used as input parameters (integral values of the fluxes of the listed particles) for further calculations of the yields of electro-, neutron, and photofission of actinides ^{232}Th, ^{238}U, ^{239}Pu. Simulations were carried out for three sample irradiation schemes: converter, converter + filter, and direct (in the absence of converter and filter).

2. Materials and Methods

2.1. Program Simulation

The application was developed for modeling the spectra of photons, residual electrons, and secondary photoneutrons, which were formed during the interaction of electrons with the converter, the combination of the converter and the filter, and hit the studied actinide samples, installed perpendicular to the beam axis of the primary electron beam [18,21,22]. The application allowed the establishment of the modeling geometry, namely the presence of converters (electron-to-photon converters) and filters for forming a bremsstrahlung beam, as well as actinide samples, taking into account their location in three-dimensional space. This made it possible to reproduce actual irradiation schemes of the studied actinide samples for implementation on electronic accelerators (in this case, on the electronic accelerator of the IEP NAS of Ukraine - the M-30 microtron [22]). When performing the calculations, the program takes into account the design features and dimensions of the M-30 microtron's electron beam output unit [15].

The program was implemented in C++ using the GEANT4 10.7.1 class library [24]. The choice of the indicated toolkit was determined by its suitability for modeling the processes of formation of various types of particles and their interaction with the studied samples on electronic accelerators [18,21,25].

The program was created for the Windows platform using multi-threading mode. A computer with a 6-core Intel (R) Core (TM) i7-9750H processor (2.60 GHz) and 36 GB of RAM was used for simulation. With the specified material base, simulations were made for the number of 1E8-1E9 events. The average run time for modeling a scheme was ~ 8-10 hours.

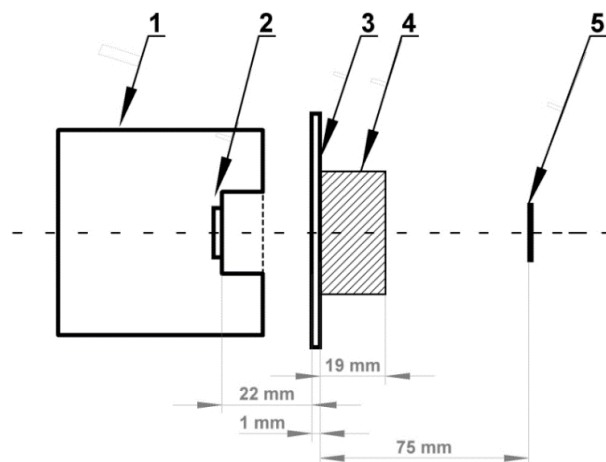## 2.2. Actinides Activation Schemes

Figure 1. Actinide stimulation scheme on the M-30 microtron electron accelerator

Simulations were made for the initial energy of electrons – 17.5 MeV. The output electron beam had the shape of an ellipse with axes of 22 × 6 mm and an equal probability distribution (taking into account the design features of the electron output node - a titanium window with a thickness of 0.05 mm) [15,18]. Figure 1 shows the scheme of stimulation of the photofission reaction of actinides on the M-30 microtron [22], where 1. is the output node of the M-30 microtron; 2. – Ti window (thickness 50 μm); 3. – Ta converter (thickness 1 mm); 4. – filter made of B$_4$C

(diameter – 35 mm, thickness – 19 mm); 5. – a sample of actinide (circle shape with a radius of 5.6 mm). The distance from the output node to the tantalum (Ta) converter was 22 mm.

Simulations of the spectra of photons, residual electrons, and secondary photoneutrons were carried out for three activation schemes of actinide samples: converter, converter + filter, and direct (when the electron beam directly interacted with the sample).

2.3. Calculation of the Outputs of Electro-, Photo- and Neutron Fission Reactions of Actinides

To assess the contribution of concomitant nuclear reactions to the photofission of actinides ([232]Th, [238]U, [239]Pu), for each of the three schemes, the yields of reactions stimulated by photons, electrons, and photoneutrons during the irradiation time of 0-10 hours were calculated separately using formula

$$Y(t) = Nt \int_{E_{th}}^{E_{max}} \varphi(E, E_{max}) \sigma(E) dE \qquad (1)$$

where $Y(t)$ is the number of actinide fission acts; N is the number of actinide nuclei in the studied sample; t – sample irradiation time; $\varphi(E, E_{max})$ – particle flux density (photons, electrons, photoneutrons), with energy E; $\sigma(E)$ – value of reaction cross sections with energy E; E_{th} – threshold energy of reactions; E_{max} – maximum spectra energy.

The calculations took into account the pulse character of the accelerator's electron beam [26, 27]. The duration of the M-30 microtron beam current pulse was 0.15 - 0.20 μs with a pulse repetition frequency of 1 kHz [28]. Based on [27] a computer program "NPMA Reaction Yield Version 1.0.2301" [29] was created to carry out calculations of the reaction yield. The application can be installed and run for a wide range of platforms (provided in formats: MSI – installation file for Windows platforms, DMB – installer file for MacOS platforms, RMP – installer file for Linux platforms, JAR – Java archive format for running under the JVM virtual machine), which support the JVM. They can be used by a wide range of end users, as they do not require large computer computing resources.
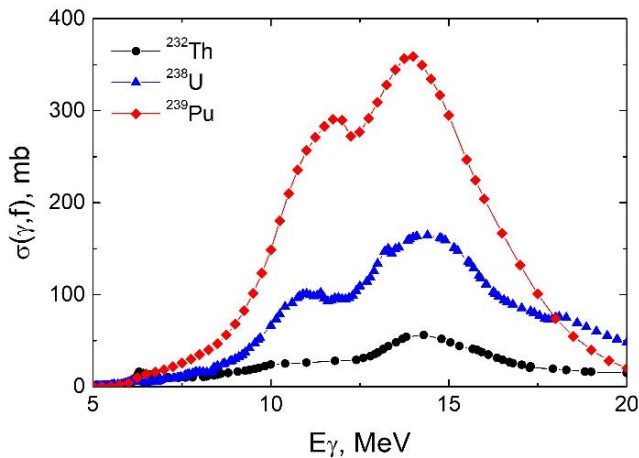

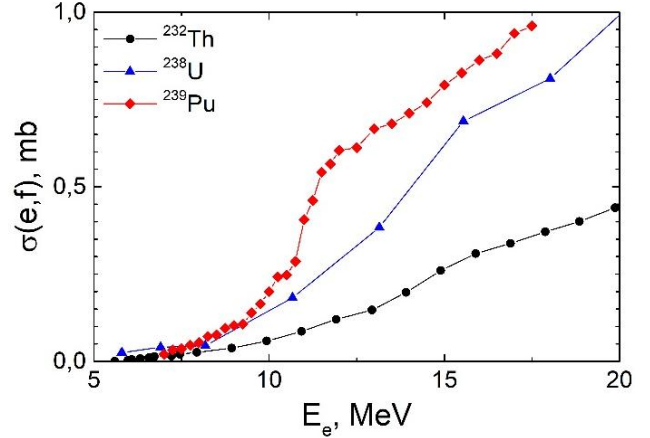**Figure 2.** Cross-sections of the photofission reaction of actinides [232]Th, [238]U, [239]Pu [30]

Figure 3. Cross-sections of the electrofission reaction of actinides [232]Th [31], [238]U [32], [239]Pu [33,34]

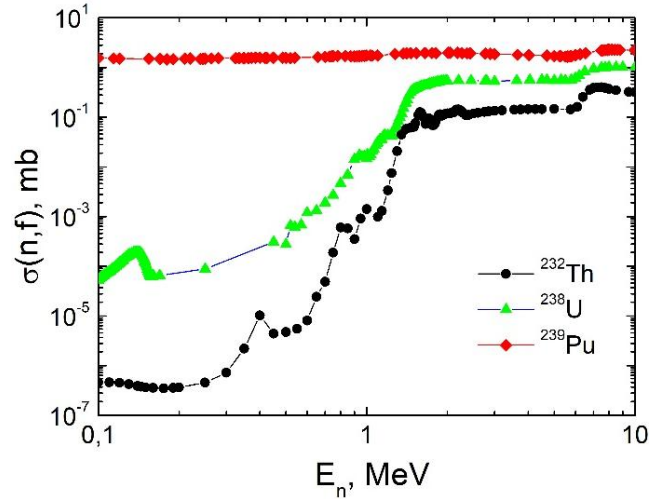**Figure 4.** Cross-sections of the neutron fission reaction of actinides [232]Th, [238]U, [239]Pu [30]

The figures show cross-sections of nuclear reactions of photofission (Fig. 2), electrofission (Fig. 3), and neutron (prompt) fission (Fig. 4) for actinides [232]Th, [238]U, and [239]Pu, which were used in calculating the yields of concomitant reactions.

ENDF library of estimated nuclear data [30] was used as input data for actinide photo- and neutron fission calculations.

To calculate the yields of electrofission reactions, experimental cross-section values from thresholds up to 17.5 MeV were taken from original works: [31] for [232]Th and [32] for [238]U. In the case of [239]Pu, interpolated values calculated from experimental data from works [33,34] were used.

3. Results and Discussion

As a result of the simulations, spectra were modeled for photons, residual electrons, and photoneutrons interacting with actinide samples. Panel Figure 5 presents the results of simulations of the spectra of bremsstrahlung photons (A), residual electrons (B), and photoneutrons (C) for three cases

of stimulation: direct, with a converter, and a combination of a converter and a filter.
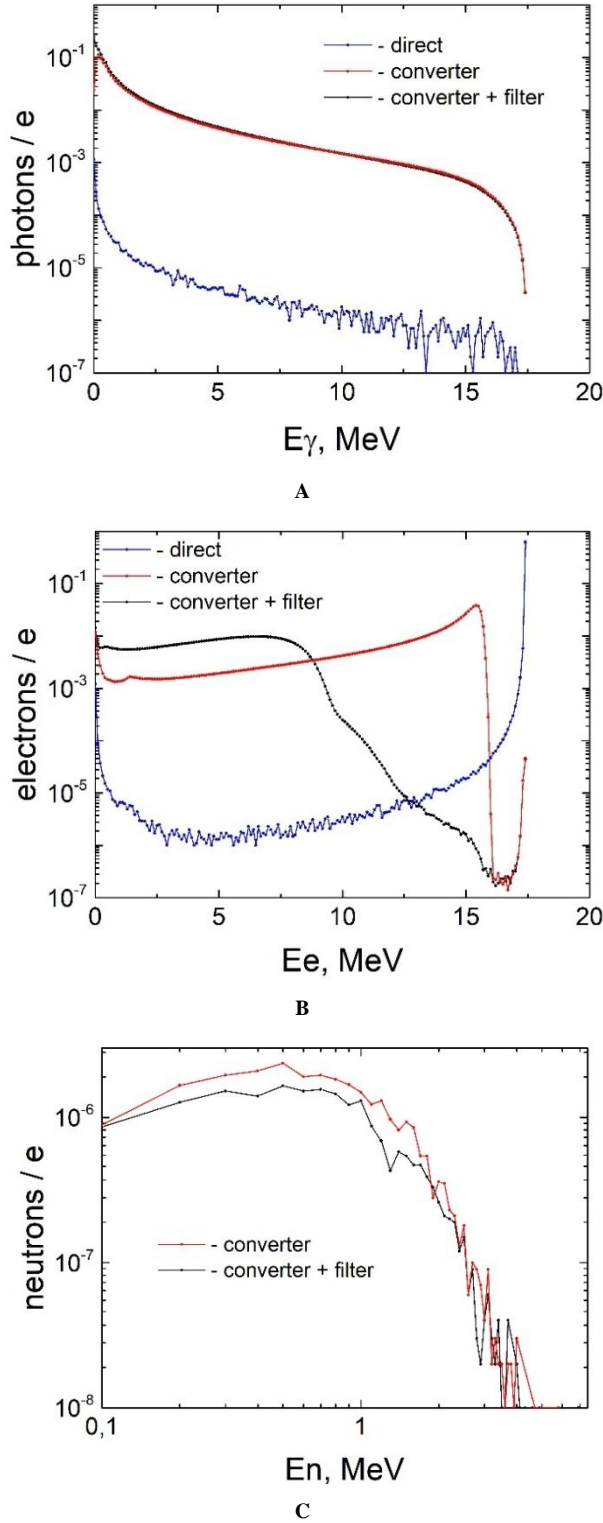
The obtained values were used to calculate the yields of photo- and electro-nuclear reactions. Similarly, integral values for photoneutron spectra (prompt) were calculated for the specified stimulation schemes. For comparison, integral values of the electron beam with energy from 6 to 17.5 MeV were also calculated for direct actinide stimulation schemes.

A

B

C

Figure 5. Spectra of bremsstrahlung photons (A), residual electrons (B), and photoneutrons (C) stimulating actinide fission reaction

The integral values of the spectra of photons and residual electrons with energies from 6 to 17.5 MeV, which stimulate the photofission and electrofission reactions of actinides, were calculated for the converter and converter + filter cases.
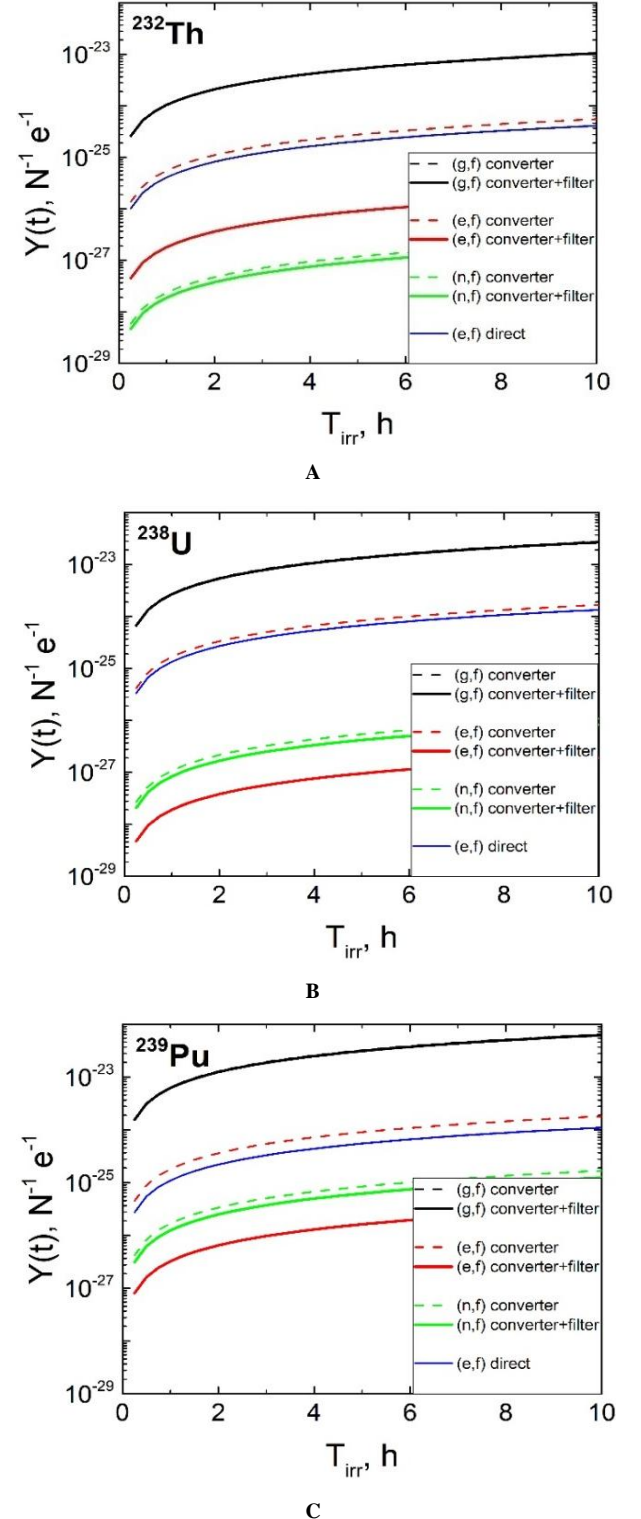

A

B

C

Figure 6. Dependence of the yields of actinide fission reactions ^{232}Th (A), ^{238}U (B), ^{239}Pu (C) on the activation time (0-10 h) for three stimulation schemes

Panel Figure 6 presents the calculated values of the dependence of the yields of the reactions of photo-, electro-, and neutron fission of the actinides ^{232}Th (A), ^{238}U (B), and ^{239}Pu (C) (reduced to one nucleus of the actinide sample and normalized to one electron emitted by a microtron) from the time of their activation. The specified dependencies are given for three activation schemes: direct, converter, converter + filter.

Calculated yields of photofission (γ,f), electrofission (e,f), and neutron fission (n,f) reactions of actinides and their contribution (numerical and percentage) to the overall result for cases: converter; converter + filter are presented in Tables 1 and 2, respectively.

Table 1. Contributions of accompanying nuclear reactions for the scheme: converter

Nuclei	(γ,f)	%	(e,f)	%	(n,f)	%
Th	3.20E-24	95,047	1.66E-25	4,932	7,13E-28	0.021
U	8,30E-24	94,282	5.00E-25	5,682	3.25E-27	0.037
Pu	1.94E-23	97,020	5.44E-25	2,726	5.08E-26	0.254

Table 2. Contributions of accompanying nuclear reactions for the scheme: converter + filter

Nuclei	(γ,f)	%	(e,f)	%	(n,f)	%
Th	3.14E-24	99,809	5.44E-27	0.173	5.68E-28	0.018
U	8.04E-24	99,962	5.73E-28	0.007	2.51E-27	0.031
Pu	1.88E-23	99,748	9.77E-27	0.052	3.76E-26	0.200

It was established that during the activation of actinides ^{232}Th, ^{238}U, and ^{239}Pu according to the scheme with a converter, the percentage contribution of electrofission is 4.932%, 5.682%, 2.726%, neutron fission - 0.021%, 0.037%, 0.254%, respectively.

For the converter + filter scheme, the percentage contribution of electrical fission is 0.173%, 0.007%, 0.052%, neutron fission - 0.018%, 0.031%, 0.2%, respectively.

The obtained data indicate that the use of the converter + filter scheme for the activation of actinide samples reduces the yields of electrofission reactions in comparison with the scheme without a filter by approximately 2 orders of magnitude. At the same time, the presence of a filter practically does not affect the yields of photofission reactions.

For fission reactions of actinides initiated by (prompt) photoneutrons, the yields when using the filter are reduced by ~20% for ^{232}Th, ~23% for ^{238}U, and ~26% for ^{239}Pu.

Additionally, calculations were made of the actinide electrofission reaction yields for the case of a direct electron beam (in the absence of a converter and filter). The results of these calculations were compared with the case of electrofission initiated by residual electrons (for the scheme - converter + filter). The numerical values of yields for both cases and the ratio of an indirect scheme yield to a direct scheme yield are given in Table 3.

The use of the converter + filter actinide activation scheme allows for the reduction of the contribution of fission reaction stimulated by residual electrons by ~ 95-99% compared to the contribution of electrofission for the direct sample activation scheme.

Table 3. Comparison of the output values of the electrolysis reaction for direct and indirect activation (converter + filter)

Nuclei	Direct	Indirect	Ratio, %
Th	1.23E-25	5.44E-27	4.417
U	4.03E-25	5.73E-28	0.142
Pu	3.32E-25	9.77E-27	2.947

As a result of the simulations, it was established that the use of the converter + filter actinide activation scheme [22] reduces the output of concomitant nuclear reactions, which are additionally initiated during the stimulation of the photofission reaction on the M-30 microtron.

Thus, the specified scheme allows stimulation of photofission reactions of actinides ^{232}Th, ^{238}U, and ^{239}Pu practically without the contribution of the indicated reactions.

4. Conclusions

As a result of the simulations and calculations, the contribution of the concomitant nuclear reactions of electro- and neutron fission to the photofission of actinides ^{232}Th, ^{238}U, ^{239}Pu during their activation at the electron accelerator - microtron M-30 for a fixed initial electron energy of 17.5 MeV was established.

The results of the calculations confirmed the effectiveness of using the proposed actinide photofission stimulation scheme on the M-30 microtron [22] to study their characteristics.

The obtained results can be used for the development of actinide activation schemes for various types of electron accelerators in the study of their nuclear-physical characteristics.

Also, the results of the calculations can be used to solve a wide range of applied problems related to the use of electronic accelerators, namely, to develop schemes for photo-activation analysis of the isotopic composition of fertile and fissile nuclear materials, alternative production of medical radioisotopes, analysis of actinide content in environmental samples, etc.

Funding

REFERENCES

[1]   Zilges A., Balabanski D.L., Isaak J., Pietrall N., Photonuclear reactions — From basic research to applications, Progress in

Particle and Nuclear Physics, 2022, v.122, Article No. 103903.

[2]   Csige L., Filipescu D.M., Photofission Studies: Past and Future in Tanihata, I., Toki, H., Kajino, T. (eds) Handbook of Nuclear Physics, Springer, Singapore, 2022.

[3]   Pylypchynets I.V., Parlag O.O., Maslyuk V.T., et al., Isotopic identification of photofissed nuclear materials in stainless steel containers using delayed gamma-rays, Problems of Atomic Science and Technology, 2022, v.141(5), p. 103-109.

[4]   Foley A., Yang H., Short-lived photofission product yields from [232] Th and [238] U at Bremsstrahlung X-ray endpoint energies of 8, 14, and 20 MeV for nuclear forensics isotope production applications, Nuclear Instruments and Methods in Physics Research Section A, 2021, v. 1013, Article No. 165621.

[5]   Dikiy N.P., Dovbnya A.N., Lyashko Yu.V., Uvarov V.L., Research of transmutation of products of nuclear cycle at the electron accelerator, Problems of atomic science and technology, 2004, v.42(1), p. 203-205.

[6]   Stoulos S., Fragopoulou M., Vagena E., et al., Electron accelerator driven system for transmutation studies, J. Rad. Nucl. Chem., 2018, v. 318, p. 1209-1217.

[7]   Nunes B.S., Rodrigues E.R.F., Fruscalso J.A.P., et al., Highly Enriched Uranium-Free Medical Radioisotope Production, Methods: An Integrative Review, Appl. Sci., 2022, v.12, Article No. 12569.

[8]   Brown M.A., Karslyan Y., Servis A.G., et al., Separation and purification of Mo-99 produced from natural U_3O_8 targets via photofission, Technical Report ANL-21/69. 2021-12-01. Argonne National Lab. (ANL), Argonne, IL (United States). https://publications.anl.gov/anlpubs/2022/01/172849.pdf.

[9]   Paschoa A.S., Arruda-Neto J.D.T., Electrofission and photofission as tools to measure actinides in environmental and biological samples, J. Radioanal. Nucl. Chem., 1992, v.156 (2), p. 297-311.

[10] Delarue M., Simon E., Pérot B., et al., Measurement of cumulative photofission yields of [235]U and [238]U with a 16 MeV Bremsstrahlung photon beam, Nuclear Inst. and Methods in Physics Research A, 2021, v.1011, Article No. 165598.

[11] Parlag O.O., Maslyuk V.T., Oleynikov E.V., et al., Structure of mass-yield distributions of [232]Th photofission product by bremsstrahlung at energy 17.5 MeV, Uzhhorod University Scientific Herald. Series "Physics", 2021, v.45, p. 50-60.

[12] Morse D.H., Antolak A.J., Doyle B.L., Photofission in uranium by nuclear reaction gamma-rays, Nuclear Instruments and Methods B, 2007, v.261(1-2), p. 378-381.

[13] Kahane S., Wolf A., Photofission of [238]U with neutron-capture gamma rays, Phys. Rev. C, 1985, v. 32, p. 1944-1955.

[14] Krishichayan, Bhike M., Howell C.R., et al., Fission product yield measurements using monoenergetic photon beams, Phys. Rev. C, 2019, v.100, Article No. 014608.

[15] Pylypchynets I.V., Parlag O.O., Masluyk V.T., et al. Double-layer targets for forming the beams of the high-energy photons on the electron accelerator of the M-30 microtron, Uzhhorod University Scientific Herald. Series "Physics", 2019, v.45, p. 50-60. (In Ukrainian).

[16] ESTAR Database.https://physics.nist.gov/PhysRefData/Star/Text/ESTAR.html.

[17] Sari A., Characterization of photoneutron fluxes emitted by electron accelerators in the 4–20 MeV range using Monte Carlo codes: A critical review, Applied Radiation and Isotopes, 2023, v. 191, Article No. 110506.

[18] Pylypchynets I., Optimal scheme for stimulating photofission of shielded nuclear materials on the Microtron M-30: a combination of theoretical and experimental studies, Scientific Herald of Uzhhorod University Series "Physics", 2022, v.52, p. 16-26.

[19] Paschoa A.S., Comparison between neutron-induced and photon-induced fission for measuring actinides, J. Radioanal. Nucl. Chem., 1994, v. 182, p. 149-155.

[20] Semisalov I., Skakun Ye., Kasilov V., Popov V., Activation technique of astrophysical photonuclear reaction rate measurements using bremsstrahlung, Problems of Atomic Science and Technology, 2014, v. 93(5), p. 102-110.

[21] Oleinikov E., Pylypchynets I., Parlag O., Computer simulation of absorption characteristics of B_4C to the components of the bremsstrahlung spectrum of the M-30 microtron, Book of abstracts of the International Conference of Young Scientists and Post-Graduate Students, Uzhhorod, 2023, p. 21-22. (In Ukrainian). Available: http://www.iep.or g.ua/content/conferenc/iep_2023/files/Book_of_abstracts_ie p2023.pdf.

[22] Oleinikov E., Pylypchynets I., Parlag O., Simulation of the optimal scheme for stimulating actinide photofission on the M-30 microtron at 17.5 MeV bremsstrahlung energy, Journal of Nuclear and Particle Physics, 2023, v.13, p. 7-16.

[23] Khabaz R., Effect of each component of a LINAC therapy head on neutron and photon spectra, Applied Radiation and Isotopes, 2018, v.139, p. 40-45.

[24] GEANT4 10.7 (4 December 2020). https://geant4.web.cern.ch/support/download.

[25] Oleinikov E., Pylypchinets I., Simulation of bremsstrahlung spectra for the M-30 microtron using the GEANT4 toolkit, Book of abstracts of the XXVII Annual Scientific Conference of the Institute of Nuclear Research of the NAS of Ukraine, Kyiv, 2021, p. 134-135 (in Ukrainian). Available: http://www.kinr.kiev.ua/kinr-2021/Book_of_Abstracts_2021.pdf.

[26] Carasco C., Eck D., Geslot B., et al., Photofission delayed gamma-ray measurements in a large cemented radioactive waste drum during LINAC irradiation, Nuclear Instruments and Methods in Physics Research Section A, 2023, v. 1053, Article No: 168360.

[27] Sun Z., A new equation for activity calculation in pulse irradiation: derivation, simulation, and experimental validation, NUCL SCI TECH, 2018, v. 29, Article No: 0123456789.

[28] Romanyuk M.I., Gaynish J.J., Turhovsky O.M., et al., Methods of formation and control of radiation fields of M-30 microtron, Journal of Physical Studies, 2022, v. 26, Article No: 1201.

[29] Certificate of copyright registration for work No. 121291 dated August 15, 2023 (Ukraine).

[30] Evaluated Nuclear Data File (ENDF). Database Version of

2022-04-22. https://www.nds.iaea.org/exfor/endf.htm.

[31] Arruda-Neto J.D.T., Rigolon W., Herded S.B., Evidence for the Statistical Fission Decay of the Giant Quadrupole Resonance of 232Th, Physica Scripta, 1987, v.35, p. 427-431.

[32] Kneissl U., H. Ströher H., Fischer R.D., et al., Investigation of the fission decay of the GQR in 238U by e-- and e+- induced fission, and tests of DWBA virtual photon spectra. in David P., Mayer-Kuckuk T., van der Woude A. (eds) Dynamics of Nuclear Fission and Related Collective Phenomena. Lecture Notes in Physics, 1972, v.158, p. 268-277.

[33] Arruda-Neto J.D.T., Yoneama M.-L., Dias J.F., et al., Electrofission of 239Pu in the energy range 7–12 MeV, Phys. Rev. C, 1997, v.55(5), p. 2471-2481.

[34] Kuznetsov V.L., Nedorezov V.G., Nikitina N.V., et al., Electron induced fission of the 238U, 237Np, 239Pu and 243Am nuclei in the energy region 100–1000 MeV, Nuclear Physics A, 1982, v. 38 (3), p. 472-486.